Appl. Magn. Reson. 28, 29–40 (2005)

Applied Magnetic Resonance

NMR Study of Tomato Pericarp Tissue by Spin–Spin Relaxation and Water Self-Diffusion

F. P. Duval, M. Cambert, and F. Mariette

Cemagref, UR Technologie des Equipements Agroalimentaires, Rennes, France

Received March 24, 2004

Abstract. Pericarp tissues of tomato varieties Quest and Cameron were studied by low-field nuclear magnetic resonance (NMR) at a controlled temperature of 20 °C. The spin-spin relaxation times and the water diffusion coefficients were measured with Carr–Parcell–Meiboom–Gill and pulsed field gradient multi-spin-echo (PFGMSE) NMR sequences. Four relaxing components were extracted from the spin–spin relaxation. The components with T_2 = 11 ms, T_2 = 65 ms, T_2 = 430 ms and T_2 = 1500 ms were related to the nonexchangeable protons and water proton in each cell compartment (i.e., cell wall–extracellular space, cytoplasm and vacuole, respectively). In contrast to the relative intensities, the T_2 values appeared insensitive to variety and harvest period. The difference in relative intensity was related to the size of the pericarp cell. The water self-diffusion coefficients for each cell compartment were determined simultaneously with the PFGMSE sequence. The water self-diffusion coefficients for the vacuole and cytoplasm were not affected by the harvest date or variety. However, the water self-diffusion in the cell wall–extracellular space was significantly different between the two varieties.

1 Introduction

Low-field nuclear magnetic resonance (NMR) relaxation and diffusion are becoming a promising techniques to study water dynamics and structural modifications in food products [1, 2]. In the case of vegetable and fruit, NMR relaxation and diffusion have been used to study mealiness in apples [3], to differentiate potato samples [4], study water transfer during drying and freezing [5, 6], and study membrane water permeability [7–11]. With Mn^{2+} as a probe to penetrate apple parenchyma tissues Snaar et al. [9] demonstrated that there are three spin–spin relaxation times which correspond to three water compartments of the fruit cells: vacuole, cytoplasm and cell wall–extracellular space. Water relaxation in biological tissues may have various origins, including chemical exchange from water proton and cell membrane protons [12, 13] and molecular diffusion [14]. Brownstein et al. [15] proposed an analytical model including

volume and surface (cell membrane) relaxation sink. Numerical models have also been developed [16, 17]. Relaxation can also increase if the magnetic field B_0 is not constant in the sample. This is the case for some plant tissues in which there is an air network between the cells for respiration purposes which creates an in situ magnetic field gradient [14, 18]. Chemical exchange effect and susceptibility artefacts are found to be less of a problem with low-field NMR spectrometer.

Water diffusion coefficients can be measured by NMR with pulsed field gradients [19–21] and pore size in porous systems and compartment size in cellular systems can be deduced from these measurements [22–25]. The self-diffusion experiment is based on attenuation of the water proton signal according to the magnetic field gradient strength. Although determination of self-diffusion is commonly achieved when a single relaxation component is detected, complications have been observed when water proton relaxation exhibits multiexponential behavior. The use of multi-spin-echo diffusion sequence was proposed to address this [26–29]. Van Dusschotten et al. [26] measured water diffusion coefficient for vacuoles and cytoplasm in apple parenchyma tissue and showed that a mono-echo diffusion sequence was inappropriate in the case of multi spin–spin relaxation time samples.

Spin–spin relaxation times and water coefficient diffusion measurements of tomato pericarp tissues from two varieties, Cameron and Quest, are presented here. A pulsed field gradient multi-spin-echo (PFGMSE) sequence was implemented and evaluated for this purpose.

2 Materials and Methods

2.1 Vegetable

Two tomato varieties, namely, Quest (De Ruiter) and Cameron (Syngenta), were studied. Both were supplied by the CTIFL (Centre Technique Interprofessionnel des Fruits et Légumes, France). The vegetables were picked up at early red stage (corresponding to 8–9 according to the color code from CTIFL). Two batches of vegetable were studied in 2003, one in June and the other in August, and vegetables were harvested one week before NMR measurements. The water content of all the samples was estimated by measuring differences in weight after drying in an oven at 103 °C for 24 h.

To prepare a sample from a tomato, a 1 cm thick slice was first cut perpendicularly to the pedicel axis. Then a cylinder (0.5 mm in diameter) was cut into the pericap flesh carefully avoiding the skin. After gently wiping the sample to remove water coming from the broken cells, it was put into an NMR tube and closed with a cap. Samples were prepared 5 min prior to use in order to limit dehydration. In June and August, 10 samples from 4 Cameron and 12 samples from 4 Quest tomatoes were prepared.

2.2 Chemicals

Dimethyl sulfoxide (DMSO) (Prolabo) and nickel(II) sulphate ($NiSO_4$) (Prolabo) were used as received. Distilled water (AES laboratoire) was used to prepare doped water.

2.3 NMR Spectrometer

All NMR measurements were performed on a 20 MHz Minispec Mq20 (Bruker) spectrometer equipped with a pulsed field gradient probe (maximum gradient amplitude of 4 T/m). Typical 90° and 180° pulse durations were 2 and 4 μs, respectively, without pulse attenuation, and 3.5 and 7.5 μs with a 8 dB pulse attenuation. The NMR measurements were performed at 20 and 40 °C for tomato and DMSO-water samples, respectively.

2.4 Spin–Spin Relaxation

Spin–spin relaxation time measurement T_2 of each tomato sample was performed with the Minispec CPMG (Carr–Parcell–Meiboom–Gill) sequence [30]: 15000 consecutive echoes were recorded with a time spacing of 0.4 ms between the 90° and the first 180° pulse. Spin–spin relaxation decay curves were fitted with two different methods, the maximum entropy method (MEM) [31], which provides a continuous distribution of relaxation components, and the Levenberg–Marquardt algorithm, which allows discrete solution for the fitting (Table Curve, Jandel Scientific) [32]. Moreover, no assumptions concerning the number of relaxation times are necessary with MEM, in contrast to the Levenberg–Marquardt algorithm method.

2.5 Diffusion

Pulsed field gradient spin echo (PFGSE) and PFGMSE were performed to measure diffusion coefficient D. The PFGSE is based on the Hahn echo sequence proposed by Skedjal and Tanner [33]. The time spacing between the 90° and 180° τ, the duration of the gradients δ, the time between the two gradients Δ, were 7.5, 0.5 and 7.5 ms, respectively. The self-diffusion coefficient for a single proton population is given by $I(t, k) = I_0\exp(-t/T_2)\exp(-kD)$, $k = \gamma^2 g_z^2 \delta^2(\Delta - \delta/3)$, where γ is the magnetogyric ratio of proton, t is the echo time, and g_z is the gradient pulse amplitude.

The PFGMSE sequence was a homemade sequence composed of a PFGSE part followed by 15000 180° pulses (see Fig. 1). The PFGSE part was similar to that described above, with τ_1, δ, Δ equal to 7.5, 0.5 and 7.5 ms, respectively. The spacing between the following 180° pulse $2\tau_2$ was equal to 0.8 ms. Only

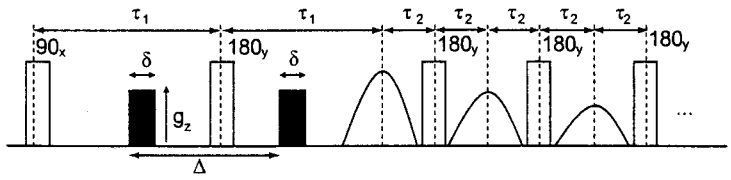

Fig. 1. PFGMSE sequence. The black and white bars correspond to the gradient and RF pulse, respectively.

the amplitudes of one out of 10 corresponding echoes were recorded. As for the PFGSE, the amplitude of the gradient pulses varied. The aim of this sequence was to distinguish different proton diffusion coefficients D_i, corresponding to different proton compartments i, of the sample. With one relaxation time and one diffusion per compartment, the amplitudes I of the recorded echoes are given by the following equation

$$I(t,k) = \sum_i I_{0,i} \exp(-t/T_{2,i}) \exp(-kD_i). \quad (1)$$

2.6 Statistical Analysis

A multifactor variance analysis (Statgraphic, Jandel Scientific) was performed to evaluate the effects of harvesting and tomato variety on both the NMR relaxation parameters and the diffusion coefficient. The significance level was set at 95%.

3 Spin–Spin Relaxation Results and Discussion

As for other biological samples, the spin–spin relaxation decay of tomato pericarp tissues was not monoexponential. Four relaxation peaks were identified by MEM on the June and August batches. An example of spin–spin relaxation distribution is given in Fig. 2. This decomposition into four components was obtained for each tomato. Nevertheless, because of heterogeneity of the pericarp tissue, some NMR signal relaxation decay was characterized by a three-exponential model. Since this behavior was rarely observed, these NMR measurements were not considered further in the analysis. No significant difference was observed for the relaxation time values and relative populations between single tomato vegetable, so average results could be calculated to describe the behavior of each variety. The average spin–spin relaxation times $T_{2,i}$ and relative intensities $I_{0,i}$ for the Quest and Cameron tomatoes are shown in Table 1 for each component (i = 0, 1, 2, 3). Multivariance analysis was performed for each compartment of the $T_{2,i}$ and $I_{0,i}$ values. There was no distinction between harvest dates or between the two varieties when only relaxation values were considered. Nevertheless, the relative amplitudes of components numbered 1, 2 and 3 exhibited significant variations according to variety and harvest date. The relative intensity

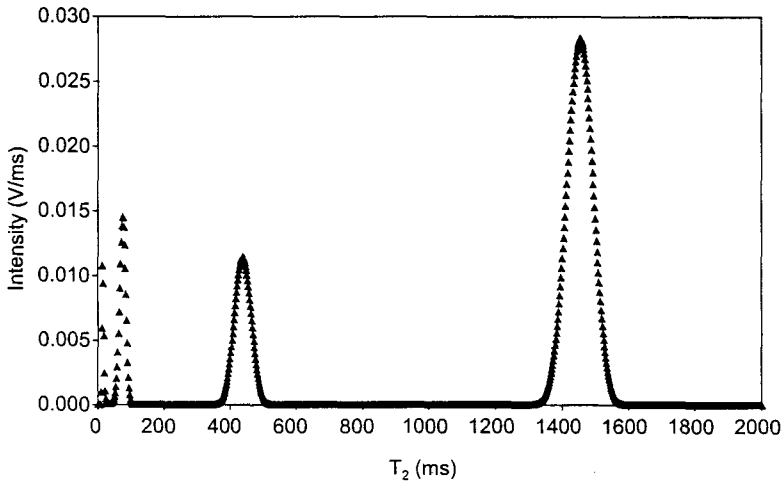

Fig. 2. Spin–spin relaxation distribution (MEM) for a Quest tomato sample, CPMG pulse spacing of 0.4 ms, $T = 20$ °C.

$I_{0,3}$ was lower for Quest than for Cameron tomatoes. $I_{0,3}$ variation between tomato varieties was compensated by variations in the relative intensity of components 1 and 2. The period effect was only significant for the Quest variety.

Multiexponential analyses were also performed with the Levenberg–Marquardt algorithm. The adjustments failed with four exponentials but residues with three exponentials were randomly distributed. The relaxation decay curve was fitted for each sample by a three-exponential model according to $I(t) = \sum_{1,2,3} I_{0,i} \exp(-t/T_{2,i})$.

Table 1. Average water content and spin-spin relaxation, with relative intensities $I_{0,0}$, $I_{0,1}$, $I_{0,2}$, $I_{0,3}$ and spin–spin relaxation time values $T_{2,0}$, $T_{2,1}$, $T_{2,2}$, $T_{2,3}$ for Quest and Cameron tomatoes by MEM. $T = 20$ °C.

Parameter	Mean (SD) for variety				Multifactor variance analysis[a]	
	Quest		Cameron		Period	Variety
	June	August	June	August		
$I_{0,0}$ (%)	2 (1)	2 (1)	2 (1)	1 (0)	n.s.	n.s.
$T_{2,0}$ (ms)	11 (4)	11 (4)	9 (3)	9 (5)	n.s.	n.s.
$I_{0,1}$ (%)	6 (2)	7 (2)	4 (1)	4 (1)	n.s.	*
$T_{2,1}$ (ms)	64 (21)	73 (14)	62 (12)	68 (13)	n.s.	n.s.
$I_{0,2}$ (%)	13 (3)	17 (2)	10 (1)	12 (1)	*	**
$T_{2,2}$ (ms)	427 (86)	432 (54)	434 (37)	429 (34)	n.s.	n.s.
$I_{0,3}$ (%)	79 (5)	74 (3)	84 (3)	83 (2)	*	**
$T_{2,3}$ (ms)	1518 (90)	1494 (71)	1524 (71)	1567 (98)	n.s.	n.s.
Total water content	95.5 (0.5)	97.2 (0.6)	96.0 (0.2)	97.3 (0.4)	**	n.s.

[a] Multifactor variance analysis (95% significance level) with high (**), low (*) and nonsignificant (n.s.) effect for relative intensities, relaxation times and water content of tomato samples.

The relaxation times and relative intensities were in good agreement between the two methods, i.e., MEM and Levenberg–Marquardt, for components 2 and 3. The two components 0 and 1 identified by MEM were artificially merged with the Levenberg–Marquardt fitting method.

This multiexponential behavior has already been observed on vegetable tissues. For apple parenchyma tissue, the CPMG relaxation decay curves were decomposed into three relaxation components and attributed to three water cell compartments [9, 26, 34, 35]. The first component, with a $T_{2,1} = 30$ ms and $I_{0,1} = 8.4\%$, was attributed to the water protons in the cell wall and extracellular space. The second component, with $T_{2,2} = 190$ ms and $I_{0,2} = 16.4\%$, was attributed to water protons in the cytoplasm. The third component, with $T_{2,3} = 1020$ ms and $I_{0,3} = 75.2\%$ was attributed to the water protons in the vacuole [9]. Some differences between the T_2 values were observed from one study to another, probably explained by the variety, ripening stage, level of dry matter, NMR measurement temperature, etc., of the apples. Van Dusschotten et al. [26] found greater relaxation time values, (1300, 380 and 50 ms at $T = 25$ °C), while Barreiro et al. [3] found smaller relaxation time values. In the latter case, the mean T_2 decreased (from around 900 to 750 ms) with increasing mealiness of apples. Four relaxation components have been extracted for potatoes [36], the first (relaxing with a $T_2 = 19$ μs) was attributed to the nonexchangeable starch protons and the other three were attributed to the water protons from the different cell compartments, including the exchangeable proton from the soluble and nonsoluble polysaccharide. Two components have been extracted in carrot parenchyma tissue [5] and attributed to the cell-wall–extracellular-space compartment ($T_{2,1} = 59.5$ ms, $I_{0,1} = 2.8\%$), and to the vacuole compartment ($T_{2,2} = 462$ ms, $I_{0,2} = 97.2\%$). More components were found as the samples were dried. This behavior was not observed in a similar study of apple parenchyma tissue [6].

According to these previous studies, we assumed that the attribution of components to the cell compartments can be extrapolated to our case. Components 1, 2 and 3 were therefore attributed to the water protons in the cell-wall–extracellular-space, in the cytoplasm and in the vacuole compartments, respectively. We assumed that the nonexchangeable proton relaxation of molecules inside the cell was described by the component labelled 0. Water protons in vacuoles, cytoplasm, and cell-wall–extracellular-space compartments hold around 80, 12 and 6% of the total NMR signal intensity, respectively. The relaxation times corresponding to each component were shorter as their water content decreased, i.e., 1500, 430, and 65 ms. Assuming this attribution, the relative amplitude change between the Quest and Cameron varieties can now be discussed. Firstly, we verified that the total NMR signal intensity per sample mass was constant for all the samples, and thus the relative intensity change could be explained by a change in the water distribution between the cell compartments. Moreover, this was in agreement with the absence of variety effect on the water content (Table 1). The relative intensity $I_{0,3}$, attributed for the water in the vacuole, was smaller for the Quest pericarp cells compared to Cameron pericarp cells. This could be due to the size of the cells. Indeed, the mean cell radius determined from optical microscopy was around 100

μm for Quest and 200 μm for Cameron (M. F. Devaux, National Institute of Food Research, Nantes, France, pers. commun.). Despite the difference in size of cells, no effect was observed on the relaxation $T_{2,3}$ value of the vacuole. Numerous studies have demonstrated that the relaxation time of water observed in a confined compartment such as a vacuole can be described as a function of the bulk T_2 ($T_{2,bulk}$), the radii of the compartment along the x-, y- and z-directions (r_x, r_y, r_z) and the net loss of magnetization at the compartment boundary, the so-called magnetization sink strength H [37]. In the case of a spherical compartment with radius r, the observed relaxation rate is given by $1/T_{2,3} = 1/T_{2,bulk} + 3H/r$.

With $T_{2,bulk} = 2$ s, the H values for Cameron and Quest were $1.1 \cdot 10^{-5}$ and $0.5 \cdot 10^{-5}$ m/s, respectively. As the $T_{2,3}$ values were identical for Quest and Cameron tomatoes, the magnetization sink strength H for Quest is smaller. In comparison, it was found to be $2.8 \cdot 10^{-5}$ m/s for maize, $4 \cdot 10^{-5}$ m/s for pearl millet [37] and $2.4 \cdot 10^{-5}$ m/s for apples [9].

4 Diffusion Results and Discussion

4.1 Validation of the PGMSE Sequence

The PFGMSE sequence was evaluated on a tube of water doped with $NiSO_4$ (2.5 mmol/l) also containing a smaller tube filled with DMSO. The proportion of water was 54.6% (g/100 g), corresponding to 63.5% of proton after correction of the respective water and DMSO proton densities. At $T = 40$ °C, diffusion coefficients and spin–spin relaxation times of the single products were measured with spin echo and CPMG, respectively. For doped water, they were $D_w = (3.08 \pm 0.02) \cdot 10^{-9}$ m²/s, $T_{2,w} = 490 \pm 5$ ms, and for DMSO they were $D_{DMSO} = (0.92 \pm 0.02) \cdot 10^{-9}$ m²/s, $T_{2,DMSO} = 2680 \pm 5$ ms. These values were compared with those found by PFGMSE on the tube containing both products. The water self-diffusion and relaxation time values were obtained from a surface function analysis of ten diffusion–relaxation curves using Eq. (1) with $i = 1, 2$. The water self-diffusion, proton population and relaxation time values were $(3.03 \pm 0.1) \cdot 10^{-9}$ m²/s, 65.0±0.1%, 485±10 ms and $(0.98 \pm 0.10) \cdot 10^{-9}$ m²/s, 35.0±0.1%, 2642±50 ms for water and DMSO, respectively. These results validated the PGMSE sequence for the determination of self-diffusion coefficients associated with specific relaxation components when spin–spin relaxation is undergoing a multiexponential behavior.

4.2 Diffusion in Tomatoes

It has previously been shown that water relaxation in tomato tissues can be modelled with three water compartments with their own relaxation times. Moreover, with PFGMSE the first echo was recorded at 15 ms, compared to 0.8 ms for CPMG. At 15 ms, the intensity of the relaxation component numbered 0 was reduced by 75%, and became nondetectable. If we assume that there is one diffusion coefficient per compartment and that exchange between compartments was

small on the time scale of the NMR experiment, then echo amplitude is given by Eq. (1) with $i = 1, 2, 3$.

$$I(t,k) = \sum_{i=1}^{3} I_{0,i} \exp(-t/T_{2,i}) \exp(-kD_i). \quad (2)$$

The PFGMSE sequence was used with 10 values of the gradient amplitude $g_z = 0$, 0.4, 0.6, 0.8, 1, 1.2, 1.4, 1.6, 1.8, and 2 T/m.

The independence of the spin–spin relaxation time value $T_{2,i}$ of the k values were first checked, then it was validated that the echo amplitude I exhibited exponential decay as a function of k according to Eq. (2). The results are illustrated for one Quest tomato sample.

Each relaxation–diffusion curve was first adjusted separately with a simple three-exponential model with k being constant,

$$I(t) = \sum_{i=1}^{3} I_{k,i} \exp(-t/T_{2,i})$$

with

$$I_{k,i} = I_{0,i} \exp(-kD_i). \quad (3)$$

Then six parameters corresponding to the relaxation times $T_{2,i}$ and diffusion-weighted amplitudes $I_{k,i}$ were estimated, and the sensitivity of the relaxation time value to k was analyzed. For all values of k, the relaxation times were constant, with only a 2% variation for the vacuole compartment (Fig. 3). For the cytoplasm and the cell-

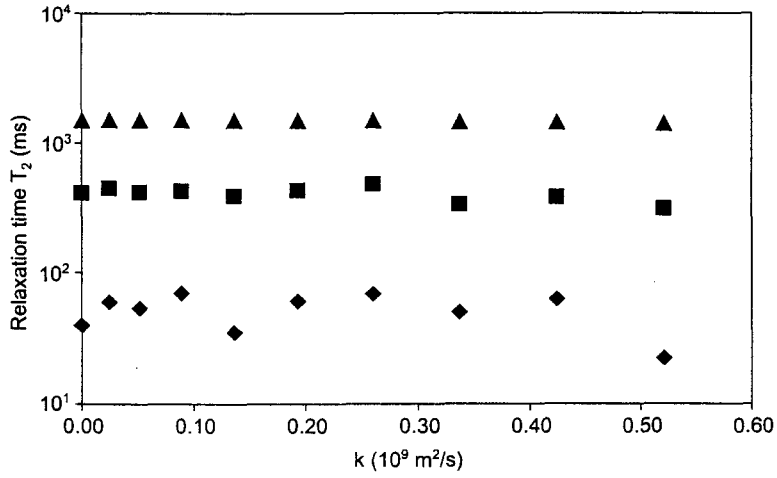

Fig. 3. Spin–spin relaxation times for a Quest tomato sample of the three cell compartments (◆, cell wall–extracellular space, $T_{2,1}$; ■, cytoplasm, $T_{2,2}$; ▲, vacuole, $T_{2,3}$) according to k for different gradient amplitudes of 0, 0.4, 0.6, 0.8, 1, 1.2, 1.4, 1.6, 1.8 and 2 T/m. The T_2 values were obtained from the fitting of the relaxation–diffusion curves one by one with amplitudes and relaxation times as adjusting parameters. $T = 20$ °C.

wall–extracellular-space compartments, the variations were greater, i.e., 13 and 30%, respectively. This was expected, since as the proton population per compartment decreased, the signal-to-noise ratio increased. The variation should be interpreted in relation to the standard deviation for the relaxation for cytoplasm and cell-wall–extracellular-space water compartments the maximum values of which were 20 and 30%, respectively. Since the variation was similar to that of the standard deviation, this confirmed that the relaxation time values were independent of the k values. Therefore, relaxation time values could be imposed in Eq. (2).

To check the exponential behavior of the signal intensity as a function of k, the relaxation time values were set using the first diffusion–relaxation curve where G equals 0 T/m. This case was chosen because the signal-to-noise ratio was greater. The relaxation times $T_{2,1}$ were slightly different from those measured with CPMG. Indeed, the first echo with PFGMSE was recorded at 15 ms compared to 0.8 ms for the CPMG. This meant that resolution for the first component was expected to be poorer. An effect from the high value of τ_1 = 7.5 ms which should induce extra signal loss can also be expected.

By adjusting one by one, the 9 other diffusion–relaxation curves as a function of time t while keeping the same $T_{2,i}$ for all k, amplitudes weighted by diffusion $I_{k,i}$, were calculated for the three compartments. On a logarithmic scale, the attenuation of the echo for each water compartment decreased linearly as a function of k and could be adjusted with Eq. (3) (Fig. 4). The assumption that only one diffusion coefficient per compartment without exchange between themselves was validated.

In the following, the water diffusion coefficients were estimated by this method. Indeed, three compartments meant nine possible adjustment parameters corresponding to $I_{0,i}$, $T_{2,i}$, D_i. With so many parameters, numerical instabilities

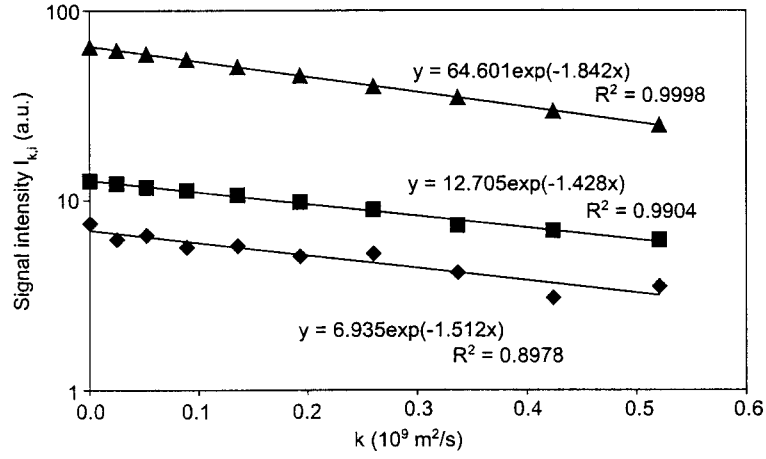

Fig. 4. Cell compartment signal intensity weighted by diffusion $I_{k,i}$ (◆, cell wall–extracellular space; ■, cytoplasm; ▲, vacuole) as a function of k for a Quest tomato sample. Solid lines are the fits by Eq. (3). T = 20 °C.

Table 2. Average water diffusion coefficients for the three cell compartments of Quest and Cameron tomato cells. $T = 20$ °C.

Diffusion coefficient	Mean (SD) (10^{-9} m^2/s^2) for variety								Multifactor variance analysis[a]	
	Quest				Cameron				Period	Variety
	June		August		June		August			
D_1	1.3	0.2	1.4	0.2	1.6	0.1	1.7	0.2	n.s.	**
D_2	1.4	0.2	1.4	0.2	1.6	0.1	1.2	0.2	n.s.	n.s.
D_3	1.8	0.1	1.9	0.1	1.8	0.1	1.9	0.1	n.s.	n.s.

[a] Multifactor variance analysis (95% significance level) with high (**) and nonsignificant (n.s.) effect for water diffusion coefficients of tomato samples.

can be expected. For this reason, the direct surface analysis of the ten diffusion–relaxation curves with Eq. (2) failed to give consistent results from one sample to another. This lack of accuracy has already been reported [26].

Table 2 shows the average values and their standard deviations corresponding to the water diffusion coefficients of the three compartments.

The vacuole compartment had a water self-diffusion coefficient ($(1.9\pm0.1)\times 10^{-9}$ m^2/s) close to that of free water ($2.0\cdot 10^{-9}$ m^2/s). This was expected as the dry matter in a vacuole is low and vacuole size is large compared to the diffusion distance probed (5 μm). Boundary effects were therefore negligible. Water self-diffusion in the cell-wall–extracellular-space and cytoplasm compartments was lower. The range of self-diffusion coefficient values was in agreement with previous results. For example, with a multi-spin echo diffusion sequence (diffusion analysis by relaxation time separated pulsed field gradient NMR), Van Dusschoten et al. [26] found $(1.4\pm0.3)\cdot 10^{-9}$, $(1.0\pm0.2)\cdot 10^{-9}$, $(1.7\pm0.2)\cdot 10^{-9}$ m^2/s for the cell-wall–extracellular-space, cytoplasm, and vacuole compartments of apple tissue at $T = 25$ °C.

No period effect was observed. Similar results were found in June and in August for the three self-diffusion coefficients. A significant difference between the Quest and Cameron varieties was observed for the self-diffusion of water in the cell wall–extracellular space. The water self-diffusion D_1 for Quest was less whatever the harvest period. There could be a correlation between this result and the magnetization sink strength. Indeed, H and D_1 were both smaller for the Quest tomato variety. Since the relaxation sink parameter had already been compared to a permeability coefficient [37], we could assume that the water transport through plasmalemma and tonoplast membranes was reduced because of common molecular composition or organisation. Consequently, water self-diffusion and relaxation NMR could be a useful technique to discriminate the molecular wall organisation or composition between different tomato varieties.

5 Conclusion

Four spin–spin relaxation components were found, three corresponding to compartments of the tomato pericarp cells. Variety and harvest period had no effect on the spin–spin relaxation time values. A significant difference between the two varieties was noted for the relative intensity of the vacuole compartment, related to size of the cell for each variety. Moreover, we demonstrated that the water compartment used for describing relaxation behavior could also be used to describe water self-diffusion. The water self-diffusion for each compartment was therefore calculated simultaneously. The water diffusion coefficient for the vacuole was the same for both varieties and close to that of free water. Cytoplasm and cell-wall–extracellular-space water diffusion coefficients were smaller than the water diffusion of the vacuole. A variety effect was detected for the water diffusion coefficients in the cell wall–extracellular space. The relaxation and diffusion experiments appear to be complementary ways to probe the water in vegetal cell compartments since no variety effect was detected for the same water compartment. The discrimination in the self-diffusion experiment was provided by the water diffusion in the cell wall–extracellular space, while for relaxation experiments the water T_2 relaxation in the vacuole was the discriminating variable. However, the structure of the membrane is proposed to explain the relaxation and diffusion properties of the two tomato varieties. Further studies will be carried out in order to analyze the composition of the wall, to relate the NMR parameters to the texture properties of the tomato and to relate the nonexchangeable proton relaxation to specific molecules.

Acknowledgements

This research was supported by the French Ministries of Research and Agriculture (Ministère délégué à la Recherche et aux Nouvelles Technologies, Ministère de l'Agriculture, de l'Alimentation, de la Pêche et des Affaires Rurales) within a Food Quality and Safety project (AQS TQ34). We thank the CTIFL for its collaboration and especially Brigitte Navez. We also thank Marie-Françoise Devaux and Marc Lahaye from INRA (Research Unit "Polysaccharides, their Organisations and Interactions") for valuable scientific discussions.

References

1. Hills B.: Magnetic Resonance Imaging in Food Science, p. 348. New York: Wiley Interscience 1998.
2. Ruan R.R., Chen P.L.: Water in Foods and Biological Materials. A Nuclear Magnetic Resonance Approach, p. 298. Lancaster: Technomic Publishing 1998.
3. Barreiro P., Moya A., Correa E., Ruiz-Altisent M., Fernandez-Valle M., Peirs A., Wright K.M., Hills B.P.: Appl. Magn. Reson. **22**, 387–400 (2002)
4. Thybo A.K., Andersen H.J., Karlsson A.H., Donstrup S., Stodkilde-Jorgensen H.: Lebensm.-Wiss. Technol. Food Sci. Technol. **36**, 315–322 (2003)
5. Hills B.P., Nott K.P.: Appl. Magn. Reson. **17**, 521–535 (1999)

6. Hills B.P., Remigereau B.: Int. J. Food Sci. Techol. **32**, 51–61 (1997)
7. Krishnan P., Nagarajan S., Moharir A.V.: Indian J. Biochem. Biophys. **40**, 46–50 (2003)
8. Velikanov G.A., Volobueva O.V., Opanasyuk O.A.: Biol. Bull. **29**, 129–134 (2002)
9. Snaar J.E.M., Van As H.: Biophys. J. **63**, 1654–1658 (1992)
10. Maheswari M., Joshi D.K., Saha R., Nagarajan S., Gambhir P.N.: Ann. Bot. (London) **84**, 741–745 (1999)
11. Zhang W.H., Jones G.P.: Plant Sci. **118**, 97–105 (1996)
12. Belton P.S., Hills B.P.: Mol. Phys. **61**, 999–1018 (1987)
13. Fedotov V.D., Miftakhutdinova F.G., Murtazin F.: Biofizika **14**, 873–882 (1969)
14. Hills B., Wright K.M., Belton P.S.: Magn. Reson. Imaging **8**, 755–765 (1990)
15. Brownstein K.R., Tarr C.E.: Phys. Rev. A **19**, 2446–2453 (1979)
16. Van der Weerd L., Melnikov S.M., Vergeldt F.J., Novikov E.G., Van As H.: J. Magn. Reson. **156**, 213–221 (2002)
17. Hills B.P., Snaar J.E.M.: Mol. Phys. **76**, 979–994 (1992)
18. Nestle N., Qadan A., Galvosas P., Suss W., Karger J.: Magn. Reson. Imaging **20**, 567–573 (2002)
19. Van As H., Lens P.: J. Ind. Microbiol. Biotechnol. **26**, 43–52 (2001)
20. Price W.S.: Concepts Magn. Res. **9**, 299–336 (1997)
21. Price W. S.: Concepts Magn. Res. **10**, 197–237 (1998)
22. Wycoff W., Pickup S., Cutter B., Miller W., Wong T.C.: Wood Fiber Sci. **32(1)**, 72–80 (2000)
23. Von Meerwall E., Ferguson R.D.: J. Chem. Phys. **74**, 6956–6959 (1981)
24. Li T.Q., Henriksson U., Klason T., Ödberg L.: J. Colloid Interface Sci. **154**, 305–315 (1992)
25. Anisimov A.V., Sorokina N.Y., Dautova N.R.: Magn. Reson. Imaging **16**, 565–568 (1998)
26. Van Dusschoten D., De Jager P.A., Van As H.: J. Magn. Reson. Ser. A **116**, 22–28 (1995)
27. Beuling E.E., Van Dusschoten D., Lens P., Van den Heuvel J.C., Van As H., Ottengraf S.P.P.: Biotechnol. Bioeng. **60**, 283–291 (1998)
28. Hurlimann M.D., Venkataramanan L.: J. Magn. Reson. **157**, 31–42 (2002)
29. Stanisz G.J., Henkelman R.M.: Magn. Reson. Med. **40**, 405–410 (1998)
30. Meiboom S., Gill D.: Rev. Sci. Instrum. **29**, 688 (1958)
31. Mariette F., Guillement J.P., Tellier C., Marchal P. in: Signal Treatment and Signal Analysis in NMR (Rutledge D.N., eds.), pp. 218–234. Amsterdam: Elsevier 1996.
32. Marquardt D.W.: J. Soc. Ind. Appl. Math. **11**, 431 (1963)
33. Stejskal E.O., Tanner J.E.: J. Chem. Phys. **42**, 288–292 (1965)
34. Snaar J.E.M., Van As H.: J. Magn. Reson. **99**, 139–148 (1992)
35. Mariette F., Rodriguez S., Lucas T., Marchal P. in: Les Produits Alimentaires et L'eau, pp. 417–422, 11ème Rencontres Agoral. Nantes: Edition Tec&Doc 1999.
36. Mariette F., Brannelec C., Vitrac O., Bohuon P. in: Les Produits Alimentaires et L'eau, pp. 411–416, 11ème Rencontres Agoral. Nantes: Edition Tec&Doc 1999.
37. Van der Weerd L., Claessens M., Efde C., Van As H.: Plant Cell Environ. **25**, 1539–1549 (2002)

Authors' address: Francois Mariette, Cemagref, UR Technologie des Equipements Agroalimentaires, CS 64426, 17 Avenue de Cucillé, 35044 Rennes, Cedex, France
E-mail: francois.mariette@cemagref.fr